Electroencephalography and Clinical Neurophysiology, 1981, 52: 257—275
Elsevier/North-Holland Scientific Publishers, Ltd.

PREVERTEBRAL (OESOPHAGEAL) RECORDING OF SUBCORTICAL SOMATOSENSORY EVOKED POTENTIALS IN MAN: THE SPINAL P_{13} COMPONENT AND THE DUAL NATURE OF THE SPINAL GENERATORS [1]

JOHN E. DESMEDT and GUY CHERON

Brain Research Unit, University of Brussels, 115, Boulevard de Waterloo, 1000 Brussels (Belgium)

(Accepted for publication: May 20, 1981)

There is a growing interest for the subcortical somatosensory evoked potentials (SEPs) to median nerve stimulation that can be recorded from the posterior surface of the neck in man (Liberson and Kim 1963; Matthews et al. 1974; Cracco and Cracco 1976; El-Negamy and Sedgwick 1978, 1979; Halliday 1978; Hume and Cant 1978; Abbruzzese et al. 1979; Symon et al. 1979; Small et al. 1980; Anziska and Cracco 1980; Chiappa et al. 1980; Cracco et al. 1980; Desmedt and Cheron 1980a; Eisen and Odusote 1980; Ganes 1980; Mauguière and Courjon 1981). The interpretation of these components is still far from clear although everyone now agrees that the positive P_9 component is a volume-conducted (far-field) potential from the afferent nerve volley near the axilla (cf., Cracco and Cracco 1976; Kimura et al. 1978; Kritchevsky and Wiederholt 1978; Desmedt and Cheron 1980a; Wiederholt 1980).

When using a non-cephalic reference electrode for recording the posterior neck SEP the onset latency of the N_{11} component was found to consistently increase by nearly 1 msec from the C7 to the C2 levels along the neck (Desmedt and Cheron 1980a) which apparently disproved the previous suggestion of a 'fixed generator' site for this wave (Matthews et al. 1974; Small et al. 1980). This point raises the important issue of the nature of the actual spinal generators involved and it has an obvious bearing on the diagnostic interpretations of spinal SEP alterations in clinical patients. We proposed that the N_{11} component was related to the volley ascending the dorsal column after spinal entry at C6-7, and anatomical relationships documented by evidence from cadaver dissections allowed a conduction velocity of 58 m/sec to be estimated for the ascending N_{11} (Desmedt and Cheron 1980a).

The present study has now replicated these results and it describes a new method for the prevertebral recording of the subcortical SEP through oesophageal electrodes in intact man. This method throws new light on current issues and provides evidence for dissociating the conducted dorsal column component from postsynaptic components locally generated in the dorsal horn.

Material and methods

After preliminary trials for elaborating the technique, 12 complete experiments were successfully carried out on 10 female and 2 male normal volunteers of 20—23 years. They were in good health, free from neurological disease, and had given informed consent. The subjects were selected from a larger group

[1] This research has been supported by grants from the Fonds de la Recherche Scientifique Médicale and the Fonds National de la Recherche Scientifique, Belgium, and by the Muscular Dystrophy Association of America.

0013-4649/81/0000—0000/$02.50

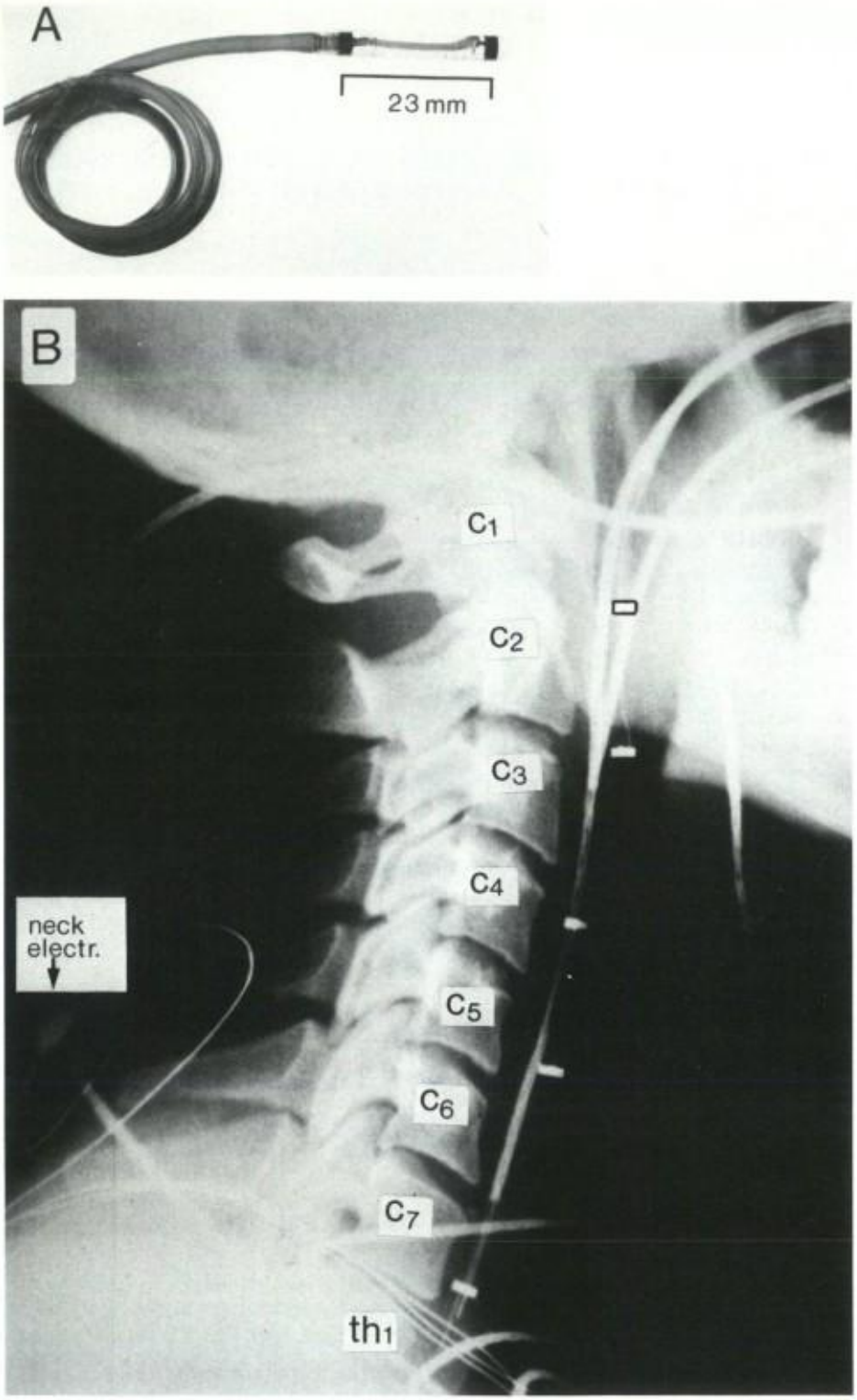

Fig. 1. A: photograph of the probe used for oesophageal recording. The two (dark) circular metal contacts on the perspex terminal are separated by 23 mm. B: lateral X-ray of the cervical spine with 6 oesophageal electrodes (3 probes each with a pair of metal strips) in place in front of the vertebrae which are labelled. A Beckman cup electrode can be seen over the spinous process of vertebra C6.

of students in the third year dental school on the basis of good yields for SEP averaging; they also had minimal tendency to vomit at probe insertion and were able to relax fully with the probes in place, so as to minimize muscle and eye blink interference. They lay comfortably on a couch in a sound-proofed, electrically shielded and air-conditioned room at 24°C.

The oesophageal probe was a flexible plastic tubing terminated by a smooth tipped perspex rod (4 mm diameter, 31 mm length) carrying in grooves at either ends two circular metal strips, 23 mm apart from each other (Fig. 1A). This probe (Disa 13K63) had been developed for intra-oesophageal recording of the electromyogram (EMG) of the diagram pillars (cf., Delhez et al. 1964). The two contacts on the probe were connected by two wires inside the plastic tubing and provided two independent active electrodes for recording against a non-cephalic reference. The probe was introduced into a nostril and passed into the oesophagus with the assistance of the subject's swallowing. Vaporization of 2% Xylocaine onto the pharynx walls helped control the gag reflex. One probe was used in 2 subjects, but 3 similar probes were simultaneously inserted to different lengths in the remaining 10 subjects, thus providing a total of 64 prevertebral recording sites. In each subject radioscopy helped adjust each probe individually to the wanted position in relation to the different vertebrae; profile and frontal X-ray prints were then made (Fig. 1B) (Desmedt et al. 1981). The probe tube emerging from the nostril was carefully fixed on the face skin with surgical tape thereby preventing any further longitudinal movement of the probe in the oesophagus with respect to the vertebrae's levels.

Each experiment included several runs with 14 simultaneous recordings that involved two 8-channel magnetic recorders both operated at 7 in./sec. Scalp, earlobes and upper neck sites were recorded from with unvarnished stainless steel needles 0.2 mm diameter. Beckman cups filled with electrode jelly were placed on the lower neck and on Erb's point above the clavicle. The non-cephalic reference was a silver plate on the dorsum of the right hand. Electrode impedance was maintained below 3000 Ω. Differential amplifiers with 10 MΩ input impedance were used. The overall bandpass extended from 2.5 kHz to 0.5 Hz (cf., Desmedt et al. 1974). For each run 1024—4096 samples were averaged off-line (4096 words of 9 bits) after editing the FM-taped data to exclude blockings, excess EMG and other interference (see Desmedt 1977, for details of methods). The bin width was 80 μsec. The analysis time was 80 msec with 1024 points for each of the 4 traces simultaneously averaged. The traces were not smoothed and were written out on an X-Y plotter. Component profiles and latencies were consistent in repeat runs on any given subject. The SEP components were labelled from their positive (P) or negative (N) polarity and their peak latency, as recommended by Donchin et al. (1977).

The stimuli were 0.2 msec square electrical pulses delivered through a pair of Beckman cup electrodes to the left median nerve (cathode proximal) just above the wrist. The intensities checked by a current probe were 3—7 mA (about 3 times subjective threshold) and elicited small thumb twitches. In some runs electrical stimuli were delivered to the peroneal nerve below the head of the fibula or to fingers through silver ring electrodes. When stimulating fingers I-II-III of the left hand, the stimulus to finger I was delayed by 0.5 msec to make up for the shorter distance to the spinal cord (Debecker and Desmedt 1964). The time intervals between stimuli were usually random and varied between 0.2 and 0.8 sec. The mean stimulation rate never exceeded 3/sec. The upper limb was warmed by infrared and its temperature was normal at 35—37°C.

Results

Latency shift of spinal N_{11} along the posterior neck

Replication of the previous results was performed on the new series of subjects. With a non-cephalic reference on the right hand, all electrodes disclosed a positive far-field P_9 which presented the same onset latency along the posterior neck and indeed also at all scalp locations. The spinal N_{11} rised from the bottom of P_9. Its mean onset latency was 9.96 ± 0.77 (S.D.) msec at the level of C6-C7 and 10.91 ± 0.77 msec at C2-C1. The two main variables affecting intersubject variability of SEP latencies in normal subjects are the tissue temperature of the stimulated arm (which was measured and maintained at 35—37°C in our studies), and the length of the arm which influences the conduction distance from wrist to cord (Desmedt 1971). We did not apply any correction for arm length since the subjects chosen had fairly homogeneous body dimensions.

The transit time between lower and upper posterior neck (Fig. 8C, D) is independent of arm length, and was found to have a mean value of 0.91 ± 0.32 msec in the new series. This figure is close to the mean transit time of 0.95 ± 0.15 msec in the previous study (Desmedt and Cheron 1980a). The latency shift along the neck is thus validated and the new mean calculated on the basis of the 18 subjects of both studies is 0.94 ± 0.24 msec. From anatomical evidence the actual conduction distance along the dorsal column was on average 55 mm from the spinal entry of median nerve afferents at C6-C7 up to the spinal C2 level (Desmedt and Cheron 1980a). The maximum ascending conduction velocity in the cord was thus recalculated as 55 : 0.94 = 58.5 m/sec.

The mean actual conduction distance from lower to upper neck is of course the best rough estimate suggested by anatomy, but it is probably no less valid than the latency shift measure. If the conduction distance was taken as 60 mm instead, the velocity would turn out as 60 : 0.94 = 64 m/sec; and if it was taken as 50 mm, the mean conduction would be 50 : 0.94 = 53 m/sec. On the other hand if the mean conduction velocity of 58 m/sec is accepted, a difference of 10 mm in the conduction distance from lower to upper neck (e.g., in larger or shorter subjects) would only result in a latency difference of 10 : 58 = 0.17 msec, a value actually smaller than the standard deviation of 0.24 msec.

Oesophageal electrodes at the level of the C7 to Th3 vertebrae

Prevertebral recordings at these levels situated below the spinal entry of the median nerve afferent volley (see spinal roots C6-C7 in stipple in Fig. 2) provided a different pattern which obviously implicates different generators. Fig. 2 presents a line drawing of a frontal X-ray with 4 recording electrodes respectively in front of the C7, Th1, Th2 and Th3 vertebrae. The averaged traces recorded from each of these electrodes against a non-cephalic reference are presented on the left column. After the initial positive deflexion, a sharp negativity was observed whose onset latency increased regularly from levels Th3 (8.2 msec) to C7 (8.8 msec) (Fig. 2A—D). A seemingly obvious (but actually wrong) move would be to attempt to calculate a conduction velocity for this negative potential by considering the vertical separation of the electrodes (60 mm from Th3 to C7) as the actual conduction distance: in this example, this would give 60 : (8.8 — 8.2) = 100 m/sec which is much too fast. The mean maximum afferent conduction velocity for the median nerve from wrist to Erb's point was 71.1 ± 4.0 m/sec in 25 young adults (Desmedt and Cheron 1980b; cf. also, Nielsen 1973). The afferent velocity is quite unlikely to suddenly accelerate by about 30 m/sec for the segment from Erb's point to cord.

For solving this problem we undertook dissections of fixed cadavers to study the geometrical relationships between the relevant spinal roots and the electrode locations in the

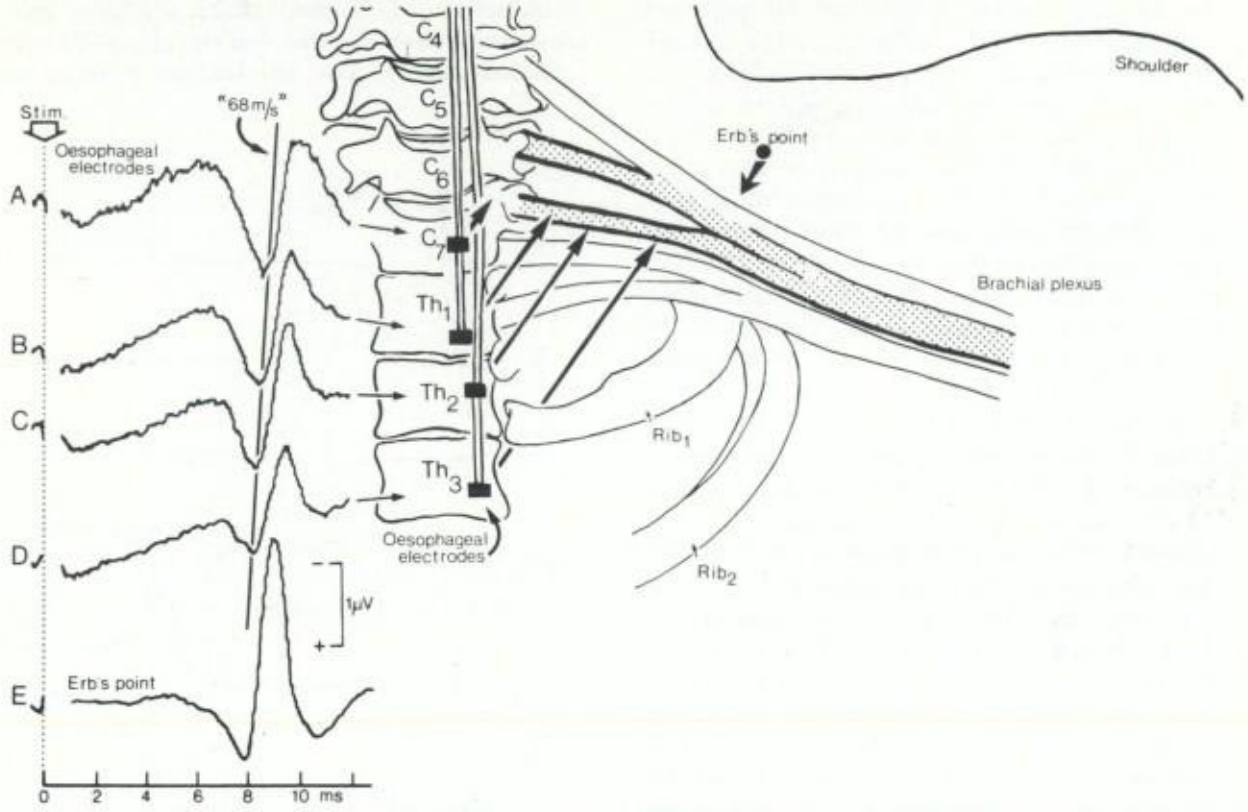

Fig. 2. Drawing from a frontal X-ray of the profiles of vertebrae C4 to Th3 with the first and second ribs. Four oesophageal electrodes (2 probes) are positioned in front of vertebrae C7 to Th3. A—D: averaged potentials elicited by the median nerve stimulus at the wrist and recorded from each of the 4 oesophageal electrodes (small arrows). In this and all subsequent figures, negativity of the active electrode registers upwards. The vertical separation of the traces is roughly proportional to the interelectrode distance. An oblique line with slope '68 m/sec' is drawn through the onset latencies of the negative potentials. E: averaged potential simultaneously recorded from Erb's point. Right side of the spine, drawing to scale of the shoulder profile and of the brachial plexus and spinal roots (C6—C7 corresponding to the median nerve afferents in stipple). This drawing is based on anatomical dissections of human cadavers and shows the true orientation of the roots with respect to the spine. The thick arrows identify the Erb's point recording site, and the presumable sites of recording of the afferent volley negativity by the oesophageal electrodes (see text).

oesophagus. The brachial plexus passes above the lateral arch of the first rib which is at the level between vertebrae C7 and Th1. Its main direction is nearly horizontal and obliquely forward. Roots C6 and C7 (carrying the median nerve afferents) run outwards with an angle of about 15° below the horizontal (Fig. 2). A useful reference to relate time with position along the plexus is provided by the Erb's point response. Like potentials recorded over peripheral nerve trunks (Gilliatt and Sears 1958), the Erb's point response is an initially positive triphasic potential (Fig. 2E) corresponding to the afferent volley approaching (positive), then passing underneath the electrode (negative), and eventually propagating beyond (positive). The anatomical location of Erb's point is well defined, between the clavicle and the anterior border of the trapezius muscle, over

the brachial plexus which can be palpated through the skin (Fig. 2). The onset of the negativity in Fig. 2E occurs at 8.0 msec and coincides with the arrival of the afferent volley at that site. Since the negativity at the oesophageal electrode Th3 starts at 8.2 msec (Fig. 2D), the latter must 'see' the afferent spike slightly more proximally than Erb's point. With an afferent conduction velocity of 71 m/sec the latency difference of $8.2 - 8.0 = 0.2$ msec would correspond to an active site about 14 mm above Erb's point (Fig. 2).

It can thus be suggested that the oesophageal electrodes, being actually at a distance of 80–20 mm from the brachial plexus, picked up the negativity of the afferent volley at levels between Erb's point and root entry into the vertebral canal, as suggested by the thick arrows joining the 4 electrodes to the roots C6-C7 in Fig. 2. If so, the actual conduction distance spanned by the Th3 to C7 oesophageal electrodes should roughly be 41 mm along the roots instead of the 60 mm corresponding to the vertical electrode separation. In this example, the root conduction velocity was recalculated as $41 : (8.8 - 8.2) = 68$ m/sec. The mean obtained in 7 subjects for electrodes between Th3 and C7 was 66.3 ± 10.9 m/sec. These values were not significantly different from the velocity of 71.1 m/sec from wrist to Erb's point.

Arrival times of the afferent volley at the brachial plexus, spinal roots and spinal cord

The above evidence suggested that, in the case of oesophageal electrodes, the first negativity was related to potentials arising, not from spinal cord, but from spinal roots. Accurate time relationships were looked into by comparing arrival times at various levels along the median nerve (Desmedt 1971; Desmedt et al. 1973) and at the spinal cord (Desmedt and Cheron 1980a). Fig. 3 illustrates sensory nerve action potentials between wrist and Erb's point (A–E) for stimulation of fingers (which excludes antidromic spikes in the motor axons of the median nerve). The conduction velocity of

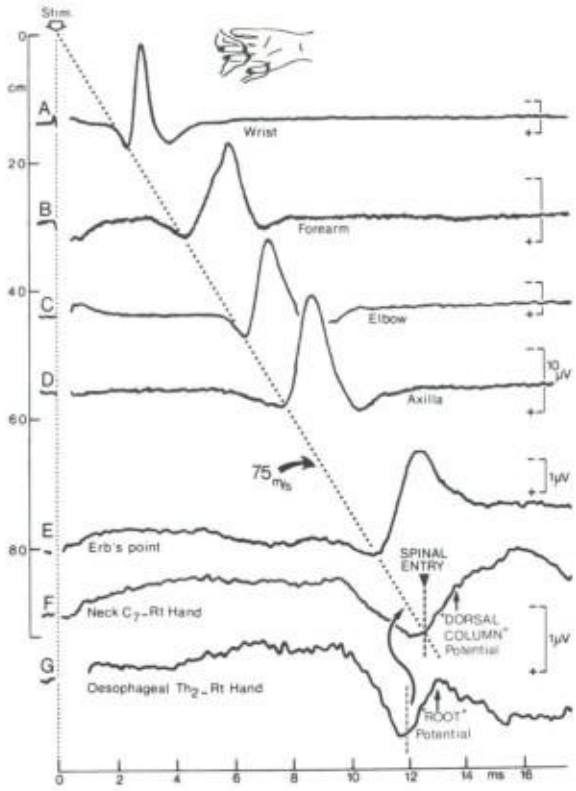

Fig. 3. Direct estimation of spinal entry time. A–E: averaged (bin width 20 µsec) sensory nerve potentials elicited by stimulation of fingers I-II-III of the left hand and recorded by needle electrodes inserted close to the nerve trunk at the wrist (A), forearm (B), elbow (C), axilla (D) and Erb's point (E). The differences in relative amplitudes at different levels depend in part on the placement of the active electrode in relation to the generator. The vertical separation of the traces is proportional to the measured distances along the nerve. The oblique dotted line passing through the onsets of negative responses corresponds to a maximum conduction velocity of 75 m/sec. Extrapolation of this linear regression to the entry of spinal roots C6-C7 into the cervical spinal cord (cf., Desmedt and Cheron 1980a, Figs. 5 and 6A) coincides with the onset of the negative spinal SEP component N_{11} recorded over the C7 spinous process (F). However, the negative potential recorded by an oesophageal electrode in front of Th2 vertebrae starts earlier (G) and it must be interpreted as a root potential.

75 m/sec calculated on these data extrapolated precisely to the onset of the N_{11} component recorded over the C7 spine at the neck, as shown by Desmedt and Cheron (1980a). However, the negativity simultaneously recorded by an oesophageal electrode in front of Th2 (Fig. 3G) started 0.6 msec *earlier* and obviously preceded the entry into the spinal cord.

Comparison of amplitudes of the positive far-field P_9 at different levels pre- or post-vertebrally disclosed consistently different trends. For oesophageal electrodes, P_9 increased from Th3 to C7 (Fig. 2A–D) and tended to diminish above C7 (Fig. 4A, B). For electrodes on the posterior neck along the midline, P_9 was small at thoracic levels and increased steadily from C7 to C2 (Fig. 4C, D) (Desmedt and Cheron 1980a). At C7-Th1, P_9 was definitely larger prevertebrally than behind (Fig. 3F, G). The data pooled for all subjects in the diagram of Fig. 4E document for the two sets of electrodes the different profiles of P_9 amplitudes which must be related to orientation of the potentials fields generated by the arriving peripheral volley.

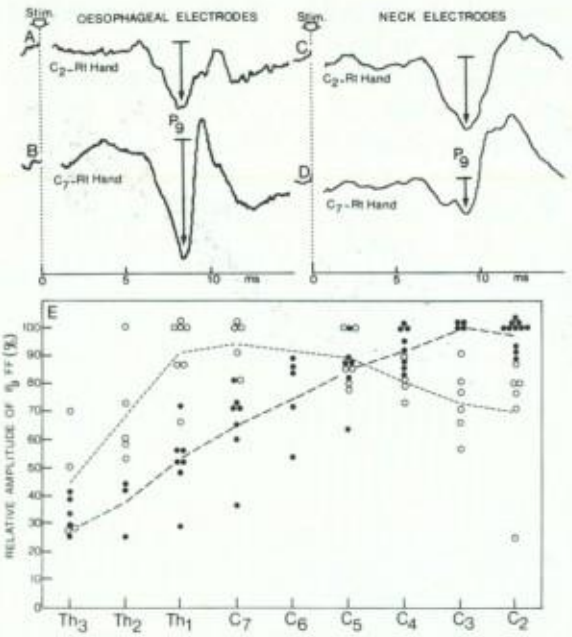

Fig. 4. Amplitude of the P_9 nerve far field at different electrode positions along the cervical spine. A, B: recordings through oesophageal electrodes in front of vertebrae C2 (A) or C7 (B) with a larger P_9 in the latter. C, D: recordings in another subject with posterior neck electrodes at C2 (C) or C7 (D): P_9 is larger over the upper spine. E: pooled data for P_9 distribution from Th3 to C2 (abscissa). The amplitudes in the ordinate are expressed for each subject in percent of the maximum P_9 recorded either pre- or post-vertebrally. There is a consistent trend for P_9 to be larger in lower neck prevertebrally (circles) and in upper neck post-vertebrally (dots).

Prevertebral recording at levels C7 to C2

Oesophageal electrodes located at or above spinal entry of the afferent volley recorded unexpected features illustrated by superimposed pre- and post-vertebral SEPs in Fig. 5A. The far-field P_9 was present with identical onset in both (Table I), but the traces differed consistently for the latency of their first negative component. The oesophageal electrode at C6 (thicker trace) recorded the spinal roots negativity with onset at 9.3 msec and peak at 10.0 msec. The posterior neck electrode saw the onset of the spinal N_{11} component at 10.0 msec which coincided both with the onset of the positive scalp far-field P_{11} (Fig. 5C, Table I) and with the spinal entry time estimated independently from conduction measures along the peripheral nerve (Desmedt and Cheron 1980a, Fig. 5; this paper, Fig. 3). The respective generators were presumably not completely segregated at either electrode sites though. The early root negativity slightly influenced the neck trace and could account in part for the bilobed bottom of P_9; conversely, a small contribution of the spinal N_{11} probably blended into, and prolonged, the prevertebrally recorded early negativity, as indeed suggested by the presence of a small negative peak (Fig. 5A, asterisk) after the roots' spike. In any case the two records diverged sharply thereafter, at 10.9 msec, with a negative N_{13} posteriorly and a positive P_{13} prevertebrally. Such a consistent phase reversal between back and front was recorded

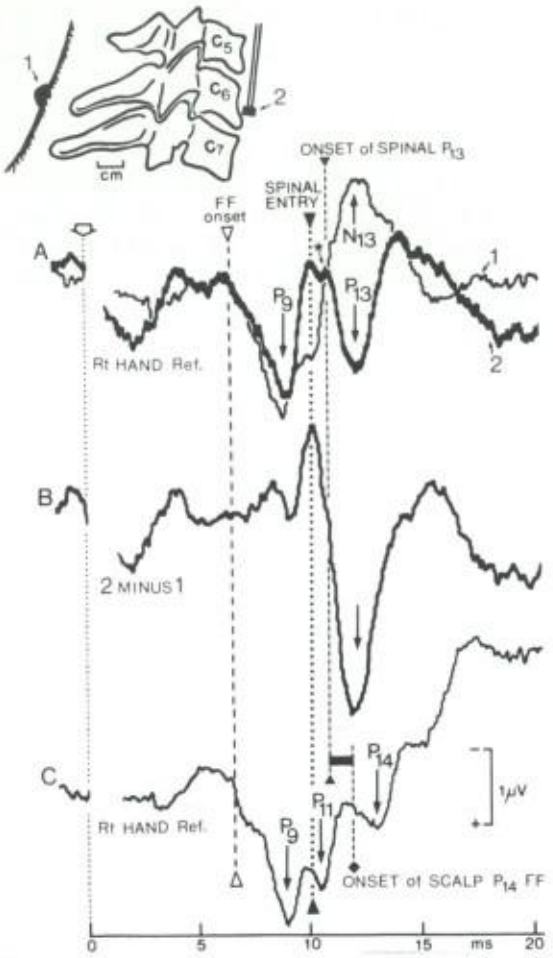

Fig. 5. A: superimposed averaged SEPs to median nerve stimulation, recorded in front (electrode 2; thicker trace) or behind (electrode 1) vertebra C6. B: subtraction of record 1 from record 2 which virtually eliminates the P_9 far field, isolates the root spike 'N_{10}', and artificially increases the P_{13} phenomenon (since the posterior N_{13} is fed into grid 2 of the amplifier). There is a clear-phase reversal between P_{13} and N_{13} in A. C: recording of cephalic far fields, P_9, P_{11} and P_{14} from the right earlobe. The vertical interrupted line indicates the onset of P_9 at 7 msec. The next vertical dotted line to the right corresponds to the spinal entry time, and to the onset of spinal N_{11} and cephalic P_{11}. The onset of P_{13}-N_{13} clearly precedes that of the P_{14} far field.

in all subjects at these cervical levels. The mean peak latency of N_{13} posteriorly was 13.10 ± 0.80 msec, and that of the prevertebral P_{13} was 13.15 ± 0.91 msec. They were not significantly different. The maximum voltage of P_{13} from onset to peak had a mean of 0.93 ± 0.45 μV (Table I).

The trace in Fig. 5B resulted from a subtraction of these two records whereby the P_9 far-field virtually cancelled out, the root spike showed up (through partial elimination of the subsequent N_{11}) and component P_{13} got much larger through the addition of the N_{13} recorded by grid 2 of the amplifier in this montage. The spinal P_{13} recorded by oesophageal electrodes presented significant differences in onset and peak latencies when compared with the scalp far-field P_{14} (Table II; Fig. 5C). The duration of the spinal P_{13} was 4.19 ± 0.64 msec and significantly exceeded the duration of the scalp-recorded far-fields P_{11} or P_{14}.

The spinal P_{13} was recorded prevertebrally between levels C7 and C3, and sharply dropped in amplitude below or above (Fig. 6B). Another important finding was the stable latency of P_{13} along the cervical spinal cord:

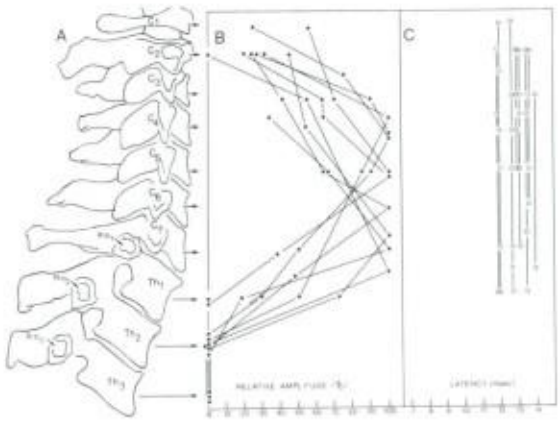

Fig. 6. Pooled data on the P_{13} phenomenon recorded by oesophageal electrodes located in front of vertebrae C1 to Th3. A: drawing of the cervical spine based on a lateral X-ray which provides the ordinate for the graphs on the right side. B: relative amplitude of P_{13} (abscissa) from its onset to its peak, expressed in percent of its maximum amplitude in each subject considered. C: peak latency of P_{13} (abscissa) in msec. Six oesophageal electrodes were used in most subjects and the measures for any given subject are joined by a line.

TABLE I

Mean values ± S.D. and *t* test by pairs for the early SEP components to median nerve stimulation in 10 subjects. N_{10} stands for the early negativity recorded by oesophageal electrodes and interpreted as a spinal root volley (Fig. 2).

	Amplitude (μV)	*t* test by pairs	Onset latency (msec)	*t* test by pairs
Prevertebral P_9 (level C6—C7)	1.53 ± 0.59	$P < 0.06$	7.12 ± 0.65	$P > 0.4$
Posterior neck P_9 (level C4)	1.15 ± 0.22	$P > 0.4$	7.04 ± 0.66	$P > 0.4$
Scalp P_9	1.02 ± 0.31		7.12 ± 0.65	
Prevertebral N_{10} (level Th2-Th3)	—		9.13 ± 0.63	$P < 0.001$
Posterior neck N_{11} (level C6-C7)	—		10.06 ± 0.81	$P > 0.6$
Scalp P_{11} far field	—		10.09 ± 0.86	
Posterior neck N_{13}	0.47 ± 0.35	$P < 0.06$	11.96 ± 0.94	$P > 0.6$
Prevertebral P_{13} (level C6-C7)	0.93 ± 0.45		11.95 ± 0.94	

the peak latency of P_{13} varied in the different subjects (if only, because of slight differences in arm length) between 11.9 and 13.8 msec, but in any given subject it was remarkably stable throughout the cervical levels where it was present and no matter its relative amplitude differences (Fig. 6).

Prevertebral recording of early SEP to peroneal nerve stimulation

In contrast to the above findings, the peroneal nerve stimulation elicited a similar profile pre- and post-vertebrally. Fig. 7C shows superimposed traces in which the far-field P_{17} was followed at each lead by a negative N_{19}. The same pair of electrodes recorded the usual phase reversal between N_{13} and P_{13} for median nerve stimulation (Fig. 7B).

Supraglottic recording

Arrays of electrodes placed in 3 experiments on the anterior aspect of the neck were used for recording with a non-cephalic reference on the right hand. At some of these electrodes the SEP profiles were not unlike those seen for oesophageal electrodes. The supraglottic trace of Fig. 8B disclosed several such features: the positive far-field P_9; a negativity starting at 8.9 msec

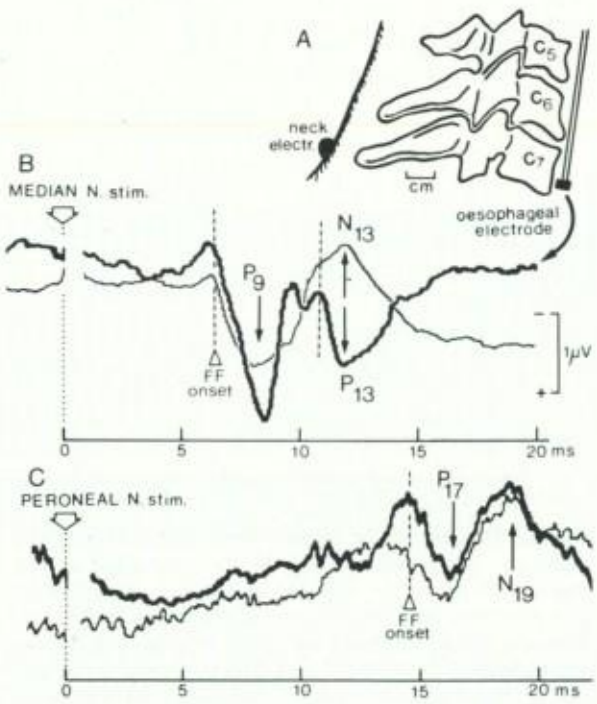

Fig. 7. Superimposed averaged SEPs recorded in front (thicker line) and behind the C7 vertebra (A), for stimulation of either the median nerve at the wrist (B) or the peroneal nerve near the head of the fibula (C). The P_{13}-N_{13} phenomenon with phase reversal occurs in B, but not in C where both traces are congruent (see text).

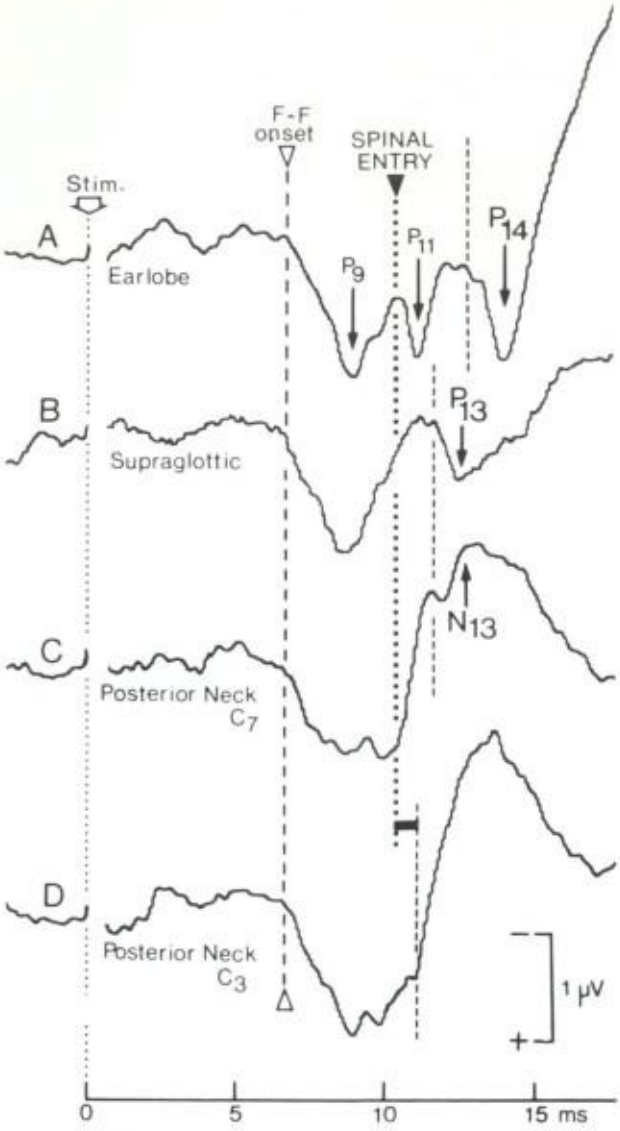

Fig. 8. Difference in onset time and duration of between the cephalic far-field P_{14} (recorded at the right earlobe, in A), and the spinal P_{13} (recorded in this example over the skin of upper neck, in B). P_{13} shows a phase reversal with the N_{13} recorded over the posterior neck at C7 (C). The latency shift of the spinal SEP N_{11} component from lower cervical spine (C) to upper cervical spine (D) is replicated.

presumably corresponding to the spinal roots spike; and a clear P_{13} whose onset obviously preceded that of the scalp far-field P_{14} (Fig. 8A). It is also noticed that the duration of the spinal P_{13} is longer than that of the scalp P_{14}, as indicated above. It is indeed amusing that averaged traces not unlike those obtained through oesophageal electrodes can be acquired by electrodes appropriately placed on the anterior aspect of the neck: however, such skin electrodes do not allow a similar detailed analysis of the SEP components as was possible for the oesophageal recordings.

Fig. 8 also illustrates dorsal neck recordings with a bilobed P_9 nerve far-field (cf., Desmedt and Cheron 1980a, Fig. 1) and another replication of the latency shift of the spinal N_{11} which was, in this example, 0.73 msec later at C3 (D) than at C7 (C).

TABLE II

Transit times between the onset of the scalp P_9 far field or the scalp P_{11} far field (spinal cord entry time) and early SEP components to median nerve stimulation in 10 subjects (mean values ± S.D.). The negative values correspond to components that precede the time reference considered. All transits are expressed in msec.

	From onset of scalp P_9	From onset of scalp P_{11}
Prevertebral P_9 onset	0.004 ± 0.10	−2.94 ± 0.51
Posterior neck P_9 onset	−0.090 ± 0.17	−3.00 ± 0.65
Prevertebral P_{13} onset	4.83 ± 0.48	1.85 ± 0.68
Prevertebral P_{13} peak	5.99 ± 0.57	3.11 ± 0.54
Posterior neck N_{13} onset	4.83 ± 0.48	1.86 ± 0.68
Posterior neck N_{13} peak	5.94 ± 0.57	3.06 ± 0.54
Scalp P_{14} far-field onset	6.51 ± 0.92	3.49 ± 0.71
Scalp P_{14} far-field peak	7.33 ± 0.68	4.38 ± 0.55

Discussion

The oesophageal electrodes used are non-invasive and benign. The only minor problem is that the subject must have patent nasal cavities (no rhinitis) and reasonably quiet pharyngeal regurgitation reflexes. Males appear to have more difficulties than young females or patients to swallow and tolerate the probes, and to remain fully relaxed for prolonged periods. X-ray monitoring is essen-

tial for accurate electrode placements (Fig. 1). The method achieves good electrical recording conditions, without EKG or other interference, and provides strategic access to the anterior aspect of vertebral bodies C2 to TH3. The new approach thus provided to the spinal SEP generators did much more than merely elaborate the evidence currently obtained from dorsal neck electrodes, and actually raised fresh issues about the differentiation of fixed versus moving generators in the spinal cord.

Volume-conducted peripheral nerve far-field P_9

The first event elicited by median nerve stimulation is a widespread far-field positivity P_9 that is recorded with an identical latency over the entire scalp, the earlobes and the neck, provided a *non-cephalic* reference is used (Cracco and Cracco 1976; Desmedt and Cheron 1980a). The latter paper clarified the complications that can arise with the use of *cephalic* reference electrodes: for example, when a lower neck electrode is connected to grid one of the amplifier and a scalp electrode such as Pz to grid two, a spurious 'N_9' can be seen simply because the P_9 far field happens to be larger at the Pz reference than at the neck. Such observations should not be taken to imply that P_9 would reverse sign at the neck. It is generally agreed that P_9 represents a volume-conducted potential generated in the stimulated nerve proximal to the axilla (Cracco and Cracco 1976; Kritchevsky and Wiederholt 1978; Wiederholt 1980) since its onset precedes the arrival of the peripheral volley at Erb's point, but is later than the onset of the median nerve potential in the axilla (Fig. 3D—G; Desmedt and Cheron 1980a). Furthermore, P_9 persists while all subsequent SEP components are lost in the patients with traction injuries of the brachial plexus when the spinal roots have been severed (Anziska and Cracco 1980).

It is interesting to notice that the P_9 far field thus relates to the nerve volley as it enters the brachial plexus from the axilla, while the second P_{11} far field recorded from scalp has an onset that coincides with spinal entry and dorsal column volley (Desmedt and Cheron 1980a). This seems to suggest that the volley travelling in the proximal brachial plexus and spinal roots is not 'seen' as a separate scalp far-field deflection. One reason for this to happen may be that the geometrical orientation of proximal brachial plexus and roots is close to the horizontal plane (Fig. 2) and therefore put at a disadvantage for volume conduction to the top of the head (in contrast to nerve trunk at the axilla, or dorsal columns or medial lemniscus).

The early negative component

With a non-cephalic reference on the hand of the unstimulated side, all the recordings from dorsal neck electrodes present a sharp negativity rising from the bottom of the P_9 far field. This negativity N_{11} recorded over the C6-C7 cervical spines is generated by the spinal cord itself near spinal entry of the afferent nerve volley since its onset consistently coincides with the arrival of the volley as estimated from direct nerve recordings (Fig. 3A—F; Desmedt and Cheron 1980a, Fig. 5). From levels C7 to C2, this negativity presents a clear latency shift which has now been replicated in the subjects of the present study (Fig. 8C, D). The increase of the N_{11} onset latency at more rostral levels along the neck has important implications for relating this SEP component to ascending conduction of the somatosensory volley in the dorsal column. Several previous studies (Matthews et al. 1974; Small et al. 1980) missed the latency shift because of their use of a scalp Fz (instead of a non-cephalic) reference whereby the spinal potentials were spuriously distorted by the scalp far-field P_{11} injected into grid two of the amplifier in that montage. This issue was thoroughly discussed by Desmedt and Cheron (1980a) and need not be repeated. The mean transit time for the spinal N_{11} is 0.94 ± 0.24 msec in the 18 subjects of both studies. The mean

maximum conduction velocity for N_{11} is then 55 : 0.94 = 58.5 m/sec, using the actual conduction distance estimated on the basis of anatomical evidence in the previous paper. This velocity is 12 m/sec slower than that of the corresponding peripheral nerve afferents in our material. The slower conduction in the centrally directed branch of the primary afferent neuron with respect to the peripheral branch has been documented in the cat (Brown 1968; Uddenberg 1968; Loeb 1976).

We have now found that Bok (1928) indicated a maximum diameter of 13 μm for the axons in the dorsal column for the upper limb (Burdach tract) in man. Applying the conversion factor of 4.5 m/sec/μm discussed earlier (Desmedt and Cheron 1980a, p. 396; cf. also Boyd and Kalu 1979), a value of $13 \times 4.5 = 58.5$ m/sec is found which agrees with the above data. The maximum velocity of the peripheral branch of the primary afferent neurone is larger and also corresponds to the diameter of its largest fibres, namely $16 \times 4.5 = 72$ m/sec (actual mean found: 71.1 m/sec; Desmedt and Cheron 1980b).

When first looking at oesophageal recordings, we were quite surprised that the prevertebral negativity rising from the P_9 far field had an earlier onset than the N_{11} at the posterior neck (Figs. 5A and 7B). It was also unexpected that the latency changes with spinal level differed from those for the posterior N_{11}. In fact the oesophageal electrodes are quite close spatially to the cervical spinal roots that emerge just behind the vertebral bodies and run obliquely in an antero-lateral direction. Evidence has been presented that the first prevertebral negativity ('N_{10}', see Table I) is related, not to the dorsal column volley, but to the spinal roots action potentials on their way from Erb's point to entry into the spinal cord (Figs. 2 and 3). As discussed above, the recordings at prevertebral levels Th3 to C7 allow a conduction velocity to be calculated which is not significantly different from the 71 m/sec found in the median nerve. The afferent axons of the median nerve enter the cord through roots C6 and C7 (Foerster 1933, 1936; Keegan and Garrett 1948; Grisolia and Wiederholt 1980) which penetrate the vertebral canal at a level corresponding to the upper aspect of the corresponding vertebra. Spinal cord segments C6-C7 entered by these roots are actually located 10—15 mm more cephalad (Desmedt and Cheron 1980a). Therefore, the geometrical relationships are quite distinct in front and behind the vertebrae: while the posterior neck electrodes over the C6-C7 spinous processes record the earliest onset of the N_{11} component presumably generated in the dorsal column, the prevertebral electrodes at the same levels first see the incoming volley in the spinal roots, about 1 msec earlier (Table I).

The different position of these two sets of electrodes (non-cephalic reference for all) in relation to the volume-conducted peripheral nerve volley is also reflected in the differences recorded for the amplitudes of the P_9 far field at different levels (Fig. 4). Although the true onset of the N_{11} SEP component cannot be recorded prevertebrally, there is some indication that N_{11} may contribute to some extent to the oesophageal records by sustaining and prolonging the early roots' negativity (Figs. 5A and 7B).

The postsynaptic spinal generator expressed in the prevertebral P_{13}

Much of the current uncertainties in the physiological interpretations of the spinal SEPs arises from the lack of an adequate data base that would provide clues for the identification of the different generators. Published statements have been either unconvincing (overinterpretation of notches in wave form profiles) or rather tentative. The use of epidural (Shimoji et al. 1971) or intrathecal (Ertekin 1973, 1976) electrodes in man confirmed the presence of a spinal negative wave, but failed to achieve a detailed analysis because of obvious limitations (and potential hazards) of the technique, and because the

wave forms recorded varied greatly with the positions of the depth electrode tip and of the reference chosen in relation to the cord. These data cannot be easily related to the currently available spinal SEPs derived from the posterior neck with a non-cephalic reference.

The use of oesophageal electrodes in man has achieved a small breakthrough in this connection by consistently disclosing a positive component P_{13} with a mean onset latency of 11.96 msec, thus about 1.9 msec later than the spinal entry time at onset of the posterior N_{11} at the levels C6-C7 (Table I). The profile of P_{13} is clearly defined and appears as a phase reversal of the N_{13} component which is recorded at the posterior neck (Figs. 5A, 7B and 8B). There is no significant difference between the time features of the two components (Table I). The finding of the P_{13}-N_{13} phase reversal proved useful to identify the posterior N_{13} whose onset is not always clearly differentiated from the preceding N_{11}, especially at higher cervical levels (Fig. 8C, D; Desmedt and Cheron 1980a, Figs. 1 and 2).

The prevertebral P_{13} is distinct from the scalp far-field P_{14} that is now related to the volume-conducted ascending volley in the medial lemniscus (Nakanishi et al. 1978; Desmedt and Cheron 1980a; Mauguière and Courjon 1981). The duration of the spinal P_{13} is longer, 4.19 msec on average, than that of the scalp far fields P_{11} or P_{14}. Finally P_{13} has a restricted distribution along the spinal cord and its amplitude drops sharply above the C3 vertebra (Fig. 6), a finding that excludes its being generated above foramen magnum.

These results can be meaningfully related to anatomical and physiological evidence on the distribution of cutaneous afferents in the cord. After spinal entry, the large fibres of the dorsal root bifurcate in the dorsal column into an ascending branch reaching the cuneate nucleus, and a shorter descending branch; collaterals of either branches penetrate into the dorsal horn through its medio-dorsal aspects and form a.o. a dense plexus in the nucleus proprius (Cajal 1909, p. 503; Schimert 1939; Sprague and Hong Chien Ha 1964) which corresponds to the cytoarchitectonic layers IV and V described in the cat (Rexed 1954) and in man (Schoenen 1973). The density of collaterals is highest at the root level and drops in the neighbouring segments (Cajal 1909; Sterling and Kuypers 1967; Imai and Kusama 1969; Rethélyi and Szentágothai 1973).

In response to a single afferent stimulus, electrophysiological recordings from the exposed cord dorsum in cat or monkey disclose a spike (currently related to the volley in the central branch of the first neurone ascending the dorsal column), rapidly followed by a more prolonged negative wave that is interpreted as a postsynaptic activation of interneurones of the dorsal horn (Gasser and Graham 1933; Hughes and Gasser 1934; Bernhard 1952; Bonnet and Bremer 1952; Lindblom and Ottoson 1953). One or more negative waves may follow the first one which is elicited by the lowest-threshold cutaneous A-alpha-beta afferents (Beall et al. 1977; Willis and Coggeshall 1978). Intraspinal mappings with microelectrodes locate the maximum negative wave in the middle layers of the dorsal horn (Coombs et al. 1956; Fernandez de Molina and Gray 1957), more precisely in layers IV and V where many interneurones are postsynaptically activated by cutaneous input (cf., Wall 1973), and identify a corresponding area of positivity in the ventral cord (cf., Beall et al. 1977). With electrodes on the surface around the cord, Austin and McCouch (1955) found the first negative wave of the cord dorsum to decrease laterally and to invert into a positive wave on the ventral aspect of the cord. These data concur remarkably with the phase reversal we recorded post- versus prevertebrally in intact man (Figs. 5A and 7B) and suggest that the N_{13}-P_{13} SEP component is postsynaptically generated within the dorsal horn. By contrast the posterior neck N_{11} component is interpreted

as the presynaptic volley ascending the dorsal column, there being no reason to implicate spinothalamic pathways in the early SEP components (cf., Halliday and Wakefield 1963; Noel and Desmedt 1975).

Along these lines, the P_{13}-N_{13} spinal component can be related to a fixed generator in the central part of the dorsal horn. This interpretation can be substantiated by 3 findings. First, the onset latency of P_{13} is remarkably stable along the cervical spinal cord in any given subject (Fig. 6C). This time constancy would indeed be expected for a potential that is focally generated in the dorsal horn over a number of spinal segments. It offers a contrast with the latency shift of about 0.94 msec recorded for the dorsal column N_{11} over the same vertical extent.

Second, the vertical extent of P_{13} has been studied in detail for comparison with the anatomical distribution of collaterals given by the primary neurones to the dorsal horn. The density of such collaterals is expected to be highest close to root entry, thus for the median nerve afferents in spinal segments C6 and C7 which are situated behind the bodies of the C5 and C6 vertebrae (Desmedt and Cheron 1980a, Fig. 6A). The descending branch of the primary neurone sends collaterals in diminishing amounts to several segments below the root entry in the cat (Sterling and Kuypers 1967; Imai and Kusama 1969; Rethélyi and Szentágothai 1973). Déjerine and Thomas (1896) studied human autopsy material with lower brachial plexus lesion and found that degenerations in the dorsal horn extend down to the second or third dorsal segments. In first approximation, the median afferents arriving in roots C6-C7 can be expected to contribute sizeable amounts of collaterals to dorsal horn to two spinal segments above (thus up to segment C4) and below (down to Th1) the roots entry. The longitudinal location of spinal segments C4 to Th1 corresponds to the bodies of vertebrae C3 to Th1 (Desmedt and Cheron 1980a, Fig. 6A). Since the exact position of our oesophageal recording electrodes was established by X-ray (Fig. 1) and since 6 levels were simultaneously derived in most subjects, the spatial distribution of P_{13} can be established precisely (Fig. 6B). These data indeed provide an excellent correlation: the maximum amplitude of P_{13} is in front of the vertebral bodies C4 to C7, and a sharp drop in voltage occurs at C3 and at Th1.

Third, no prevertebral positive component analogous to P_{13} is recorded for afferent volleys elicited in the lower limb. The oesophageal electrode at C7 only records a first far-field P_{17} that is followed by the dorsal column negative component N_{19}, and the trace profile is virtually identical to the one recorded by the posterior neck electrode (Fig. 7C). This fits in with our hypothesis that P_{13} is related to a postsynaptic fixed generator in dorsal horn because the axons ascending from lumbosacral levels in the tract of Goll (gracilis) do not anatomically innervate the dorsal horn at cervical levels.

It is important to emphasize that the N_{13}-P_{13} spinal component thus identified is generated by a neural structure, the spinal dorsal horn (mainly layers IV and V), that is *not* a serial link in the somatosensory pathway going up from spinal entry to cerebral cortex. Therefore the N_{13}-P_{13} component recorded from the neck or oesophagus should, under certain pathological conditions, undergo dissociated changes that would not be necessarily reflected in the subsequent components generated higher up along the somatosensory pathway. There are indeed cases, for example in patients with multiple sclerosis, where this spinal component would be reduced or delayed by a focal lesion even though the cortical N_{20} component presents a latency within the normal range (cf., Small et al. 1980). We interpret this to mean that a focal lesion can involve the collateral nerve branches directed onto the dorsal horn interneurones without affecting the stem nerve fibres (central part of the primary neurone) ascending in the dorsal column that activate the lemniscal neurones at the cuneate nucleus. Our finding that the

N_{13}-P_{13} spinal component is generated in the dorsal horn and presents a longer duration than the scalp far fields emphasizes that it should be carefully distinguished from the P_{13}-P_{14} scalp far field on the basis of distinct generators, and even though the respective latencies may overlap in time. For example, in patients with a destruction of the cephalad dorsal column down to the level cervical C5, the P_{14} scalp far field is eliminated while a negative N_{13} with rather prolonged time course is recorded from the posterior neck (Mauguière and Courjon 1981). This N_{13} wave should not be interpreted as a dorsal column volley, but related instead to the dorsal horn fixed generator which can still be activated through collateral branches of the caudally directed bifurcation of the primary nerve fibre entering the spinal cord.

Summary

Short-latency somatosensory evoked potential (SEP) components to median nerve or finger stimulation were recorded in 12 normal young adults with 14 channels, using a non-cephalic reference. Several electrodes were placed along the posterior neck, earlobes and scalp while oesophageal probes provided 2—6 recording sites at known levels in front of vertebrae C2 to Th3 (Fig. 1). The oesophageal electrodes provided a new non-invasive point of entry that secured important data about the generator sources of the spinal SEP components.

All cephalic electrodes recorded a P_9 far field which is greater over the scalp, earlobes and rostral cervical spine than over the caudal cervical spine. P_9 is the volume-conducted peripheral nerve volley coursing between axilla and spinal cord. The direct recording of arrival times of the peripheral volley along the median nerve and brachial plexus (Erb's point) served to estimate the spinal entry time which coincided with the onset of the posterior neck N_{11} (at levels C6-C7) and of the scalp P_{11} far field (Fig. 3). The latency shift of the onset of N_{11} from lower to upper neck has been replicated (Fig. 8C, D) and N_{11} is interpreted as a presynaptic volley ascending the dorsal column (central branch of the primary neurone) at a velocity of 58 m/sec (Desmedt and Cheron 1980a).

At oesophageal electrodes in front of the C7-Th3 vertebrae, the first negative component starts before the spinal entry time and it corresponds to action potentials in the spinal roots (Figs. 2 and 3). The most remarkable feature of oesophageal recordings in front of the C3 to Th2 vertebrae is the positive P_{13} component which represented a phase reversal of the second negativity N_{13} recorded from posterior neck (Fig. 5). The P_{13}-N_{13} phenomenon was recorded in all subjects and presented a stable latency throughout the cervical cord (Fig. 6C). It was clearly differentiated from the scalp far-field P_{14} which is related to the ascending volley in the median lemniscus (Figs. 5 and 8; Tables I and II). The spinal P_{13} did not extend above C2 and it was obviously generated below the foramen magnum. P_{13} is interpreted as a dorsal horn postsynaptic potential which is elicited by collateral branches of the (bifurcated) primary afferent fibre.

The use of 14 simultaneous recordings including a series of pre- and post-vertebral electrodes clearly identified two distinct generators for the spinal SEP components to median nerve stimulation: a presynaptic generator which ascends the dorsal column (N_{11}) and a postsynaptic fixed generator in the dorsal horn of the cervical spinal cord (N_{13}-P_{13}).

Résumé

On a enregistré avec 14 canaux (référence non-céphalique) les composantes de brève latence du potentiel évoqué somesthésique (PES) à la stimulation du nerf médian ou des

doigts chez 12 sujets jeunes normaux. Des électrodes étaient placées sur le cuir chevelu, les lobes d'oreille et la nuque. De plus des sondes oesophagiennes permettaient de dériver en 2—6 points devant les vertèbres C2 à Th3 (Fig. 1). Ces électrodes oesophagiennes sont bien tolérées et apportent des données nouvelles importantes sur les générateurs des composantes spinales du PES.

Toutes les électrodes céphaliques ont enregistré d'abord un potentiel far-field P_9 qui est plus grand sur le cuir chevelu et jusqu'à la partie supérieure de la colonne cervicale que dans la partie inférieure de la nuque. P_9 est le potentiel de champ de la volée nerveuse périphérique entre l'aisselle et la moelle. Nous avons enregistré les potentiels de nerf médian et du plexus brachial (point d'Erb) pour évaluer le moment de l'entrée de la volée dans la moelle cervicale et ce dernier coïncide avec le début du N_{11} à la nuque (C6-C7) et du potentiel de champ P_{11} sur le cuir chevelu (Fig. 3). Nous avons confirmé l'augmentations de latence du N_{11} entre le bas et le haut de la nuque (Fig. 8C, D); N_{11} est interprétée comme la volée présynaptique montant dans la colonne dorsale à une vitesse de 58 m/sec (Desmedt et Cheron 1980a).

Au niveau des électrodes oesophagiennes se trouvant devant les vertèbres C7-Th3, la première négativité débute avant l'arrivée de la volée périphérique à la moelle et elle est interprétée comme un potentiel d'action dans les racines spinales (Figs. 2 et 3). Le phénomène le plus remarquable enregistré par les électrodes oesophagiennes se trouvant devant les vertèbres C3 à Th2 est la composante PES P_{13} qui est en phase inverse par rapport à la deuxième négativité N_{13} dérivée au niveau de la nuque (Fig. 5). Le phénomène P_{13}-N_{13} a été observé chez tous les sujets; il présente une latence stable tout le long de la moelle cervicale (Fig. 6C). Il est clairement distinct du potentiel de champ P_{14} du cuir chevelu qui lui est l'expression de la volée montante dans le ruban de Reil médian (Figs. 5 et 8; Tableaux I et II). Le P_{13} spinal ne s'étend pas plus haut que la vertèbre C2 et son générateur est de façon évidente en-dessous du trou occipital. P_{13} est interprété comme un potentiel postsynaptique dans la corne dorsale de la moelle cervicale où il est déclenché par des branches collatérales de la fibre afférente primaire (bifurquée).

L'utilisation de 14 dérivations simultanées comprenant des séries d'électrodes pré- et post-vertébrales a ainsi clairement identifié deux générateurs distincts pour les composantes spinales du PES à la stimulation du nerf médian: un générateur présynaptique qui est conduit le long de la colonne dorsale (N_{11}), et un générateur fixe postsynaptique dans la corne dorsale de la moelle épinière cervicale (N_{13}-P_{13}).

We wish to thank Prof. J. Mulnard, director of the Department of Anatomy, for his help and suggestions in relation to the studies of human anatomical material, and Prof. J. Bollaert, Chief of the Department of Radiology, for his active cooperation in the X-ray studies of oesophageal electrode placements.

References

Abbruzzese, M., Favale, E., Leandri, M. and Ratto, S. Electrophysiological assessment of the central lemniscal pathway in man. Experientia (Basel), 1979, 35: 775—776.

Anziska, B. and Cracco, R.Q. Short latency somatosensory evoked potentials: studies in patients with focal neurological disease. Electroenceph. clin. Neurophysiol., 1980, 49: 227—239.

Austin, G.M. and McCouch, G.P. Presynaptic component of intermediary cord potential. J. Neurophysiol., 1955, 18: 441—451.

Beall, J.E., Applebaum, A.E., Foreman, R.D. and Willis, W.D. Spinal cord potentials evoked by cutaneous afferents in the monkey. J. Neurophysiol., 1977, 40: 199—211.

Bernhard, C.G. The cord dorsum potentials in relation to peripheral source of afferent stimulation. Cold Spring Harb. Symp., 1952, 17: 221—232.

Bok, S.T. Das Rückenmark. In: v. Möllendorff (Ed.), Handbuch der mikroskopischen Anatomie der Menschen, 1928, 4: 478—573.

Bonnet, V. et Bremer, F. Les potentiels synaptiques

et la transmission nerveuse centrale. Arch. intern. Physiol., 1952, 60: 33–93.

Boyd, I.A. and Kalu, K.U. Scaling factor relating conduction velocity and diameter for myelinated afferent nerve fibres in the cat hind limb. J. Physiol. (Lond.), 1979, 289: 277–297.

Brown, A.G. Cutaneous afferent fibre collaterals in the dorsal columns of the cat. Exp. Brain Res., 1968, 5: 293–305.

Cajal, S. Ramón y Histologie du Système Nerveux de l'Homme et des Vertébrés. Maloine, Paris, 1909.

Chiappa, K.H., Choi, S.K. and Young, R.R. Short latency somatosensory evoked potentials following median nerve stimulation in patients with neurological lesions. In: J.E. Desmedt (Ed.), Clinical Uses of Cerebral, Brainstem and Spinal Somatosensory Evoked Potentials, Progr. clin. Neurophysiol., Vol. 7. Karger, Basel, 1980: 264–281.

Coombs, J.S., Curtis, D.R. and Landgren, S. Spinal cord potentials generated by impulses in muscle and cutaneous afferent fibres. J. Neurophysiol., 1956, 19: 452–467.

Cracco, R.Q. and Cracco, J.B. Somatosensory evoked potentials in man: far-field potentials. Electroenceph. clin. Neurophysiol., 1976, 41: 460–466.

Cracco, R.Q., Cracco, J.B., Sarnowski, R. and Vogel, H.B. Spinal evoked potentials. In: J.E. Desmedt (Ed.), Clinical Uses of Cerebral, Brainstem and Spinal Somatosensory Evoked Potentials, Progr. clin. Neurophysiol., Vol. 7. Karger, Basel, 1980: 105–117.

Debecker, J. et Desmedt, J.E. Les potentiels évoqués cérébraux et les potentiels de nerf sensible chez l'homme. Acta neurol. belg., 1964, 64: 1212–1248.

Déjerine, J. et Thomas, A. Contribution à l'étude du trajet intramédullaire des racines postérieures dans la région cervicale et dorsale supérieure de la moelle épinière. Sur l'état de la moelle épinière dans un cas de paralysie radiculaire inférieure du plexus brachial d'origine syphilitique. C.R. Soc. Biol. (Paris), 1896, 48: 675–679.

Delhez, L., Bottin, R., Damoiseau, J. et Petit, J.M. Examen comparatif des électromyogrammes des piliers du diaphragme dérivés au moyen de trois modèles de sondes-électrodes. Electromyography, 1964, 4: 5–14.

Desmedt, J.E. Somatosensory cerebral evoked potentials in man. In: A. Rémond (Ed.), Handbook of Electroencephalography and Clinical Neurophysiology, Vol. 9. Elsevier, Amsterdam, 1971: 55–82.

Desmedt, J.E. Some observations on the methodology of cerebral evoked potentials in man. In: J.E. Desmedt (Ed.), Attention, Voluntary Contraction and Event-Related Cerebral Potentials, Progr. clin. Neurophysiol., Vol. 1. Karger, Basel, 1977: 12–29.

Desmedt, J.E. and Cheron, G. Central somatosensory conduction in man: neural generators and interpeak latencies of the far-field components recorded from neck and right or left scalp and earlobes. Electroenceph. clin. Neurophysiol., 1980a, 50: 382–403.

Desmedt, J.E. and Cheron, G. Somatosensory evoked potentials to finger stimulation in healthy octogenarians and in young adults: wave forms, scalp topography and transit times of parietal and frontal components. Electroenceph. clin. Neurophysiol., 1980b, 50: 404–425.

Desmedt, J.E., Noël, P., Debecker, J. and Namèche, J. Maturation of afferent conduction velocity as studied by sensory nerve potentials and by cerebral evoked potentials. In: J.E. Desmedt (Ed.), New Developments in Electromyography and Clinical Neurophysiology, Vol. 2. Karger, Basel, 1973: 52–63.

Desmedt, J.E., Brunko, E., Debecker, J. and Carmeliet, J. The system bandpass required to avoid distortion of early components when averaging somatosensory evoked potentials. Electroenceph. clin. Neurophysiol., 1974, 37: 407–410.

Desmedt, J.E., Cheron, G. and Bollaert, J. Use of oesophageal electrodes to study ascending conduction of somatosensory volleys in the cervical spinal cord in man. Electroenceph. clin. Neurophysiol., 1981, 51: 87 P.

Donchin, E., Callaway, E., Cooper, R., Desmedt, J.E., Goff, W.R., Hillyard, S.A. and Sutton, S. Publication criteria for studies of evoked potentials: report of a committee. In: J.E. Desmedt (Ed.), Attention, Voluntary Contraction and Event-Related Cerebral Potentials, Progr. clin. Neurophysiol., Vol. 1. Karger, Basel, 1977: 1–11.

Eisen, A. and Odusote, K. Central and peripheral conduction times in multiple sclerosis. Electroenceph. clin. Neurophysiol., 1980, 48: 253–265.

El-Negamy, E. and Sedgwick, E.M. Properties of spinal somatosensory evoked potential recorded in man. J. Neurol. Neurosurg. Psychiat., 1978, 41: 762–768.

El-Negamy, E. and Sedgwick, E.M. Delayed cervical somatosensory potentials in cervical spondylosis. J. Neurol. Neurosurg. Psychiat., 1979, 42: 238–241.

Ertekin, C. Human evoked electrospinogram. In: J.E. Desmedt (Ed.), New Developments in Electromyography and Clinical Neurophysiology, Vol. 2. Karger, Basel, 1973: 344–351.

Ertekin, C. Studies on the human evoked electro-

spinogram: the conduction velocity along the dorsal funiculus. Acta neurol. scand., 1976, 53: 21—38.

Fernandez de Molina, A. and Gray, J.A.B. Activity in the dorsal grey matter after stimulation of cutaneous nerves. J. Physiol. (Lond.), 1957, 137: 126—140.

Foerster, O. The dermatomes of man. Brain, 1933, 56: 1—39.

Foerster, O. Symptomatologie der Erkrankungen des Rückenmarks und seiner Wurzeln. In: O. Bumke and O. Foerster (Eds.), Handbuch der Neurologie, Vol. 5. Springer, Berlin, 1936: 1—403.

Ganes, T. Somatosensory conduction times and peripheral, cervical and cortical evoked potentials in patients with cervical spondylosis. J. Neurol. Neurosurg. Psychiat., 1980, 43: 683—689.

Gasser, H.S. and Graham, H.T. Potentials produced in the spinal cord by stimulation of dorsal roots. Amer. J. Physiol., 1933, 103: 303—320.

Gilliatt, R.W. and Sears, T.A. Sensory nerve action potentials in patients with peripheral nerve lesions. J. Neurol. Neurosurg. Psychiat., 1958, 21: 109—118.

Grisolia, J.S. and Wiederholt, W.C. Short latency somatosensory evoked potentials from radial, median and ulnar nerve stimulation in man. Electroenceph. clin. Neurophysiol., 1980, 50: 375—381.

Halliday, A.M. Clinical applications of evoked potentials. In: W.B. Matthews and G.H. Glaser (Eds.), Recent Advances in Clinical Neurology, Vol. 2. Churchill-Livingston, Edinburgh, 1978: 47—73.

Halliday, A.M. and Wakefield, G.S. Cerebral evoked potentials in patients with dissociated sensory loss. J. Neurol. Neurosurg. Psychiat., 1963, 26: 211—219.

Hughes, J. and Gasser, H.S. Some properties of the cord potentials evoked by a single afferent volley. Amer. J. Physiol., 1934, 108: 295—306.

Hume, A.M. and Cant, B.R. Conduction time in central somatosensory pathways in man. Electroenceph. clin. Neurophysiol., 1978, 45: 361—375.

Imai, Y. and Kusama, T. Distribution of the dorsal root fibers in the cat: an experimental study with the Nauta method. Brain Res., 1969, 13: 338—359.

Keegan, J.J. and Garrett, F.D. The segmental distribution of the cutaneous nerves in the limbs of man. Anat. Rec., 1948, 102: 409—437.

Kimura, J., Yamada, T. and Kawamura, H. Central latencies of somatosensory cerebral evoked potentials. Arch. Neurol. (Chic.), 1978, 35: 683—688.

Kritchevsky, M. and Wiederholt, W.C. Short latency somatosensory evoked responses in man. Arch. Neurol. (Chic.), 1978, 35: 706—711.

Liberson, W.T. and Kim, K.C. The mapping out of evoked potentials elicited by stimulation of the median and peroneal nerves. Electroenceph. clin. Neurophysiol., 1963, 15: 721.

Lindblom, U.F. and Ottoson, J.O. Localization of the structure generating the negative cord dorsum potential evoked by stimulation of low threshold cutaneous fibres. Acta physiol. scand., 1953, 29 (Suppl. 106): 180—190.

Loeb, G.E. Decreased conduction velocity in the proximal projections of myelinated dorsal root ganglion cells in the cat. Brain Res., 1976, 103: 381—385.

Matthews, W.B., Beauchamp, M. and Small, D.G. Cervical somatosensory evoked responses in man. Nature (Lond.), 1974, 52: 230—232.

Mauguière, F. and Courjon, J. The origin of short-latency somatosensory evoked potentials in man. A clinical contribution. Ann. Neurol., 1981, 9: 707—710.

Nakanishi, T., Shimada, Y., Sakuta, M. and Toyokura, Y. The initial positive component of the scalp-recorded somatosensory evoked potential in normal subjects and in patients with neurological disorders. Electroenceph. clin. Neurophysiol., 1978, 45: 26—34.

Nielsen, V.K. Sensory and motor nerve conduction in the median nerve in normal subjects. Acta med. scand., 1973, 194: 435—443.

Noël, P. and Desmedt, J.E. Somatosensory cerebral evoked potentials after vascular lesions of the brain stem and diencephalon. Brain, 1975, 98: 113—128.

Rethélyi, M. and Szentágothai, J. Distribution and connections of afferent fibres in the spinal cord. In: A. Iggo (Ed.), Handbook of Sensory Physiology, Vol. 2. Springer, Berlin, 1973: 207—252.

Rexed, B. A cytoarchitectonic atlas of the spinal cord in the cat. J. comp. Neurol., 1954, 100: 297—379.

Schimert, J. Das Verhalten der Hinterwurzelkollateralen im Rückenmark. Z. Anat. Entwickl.-Gesch., 1939, 109: 665—687.

Schoenen, J. Etude histoenzymologique des couches cytoarchitectoniques de la moelle de différents mammifères et de l'homme. Bull. Ass. Anat., 1973, 58: 415—425.

Shimoji, K., Higashi, H. and Kano, T. Epidural recording of spinal electrogram in man. Electroenceph. clin. Neurophysiol., 1971, 30: 236—239.

Small, D.G., Beauchamp, M. and Matthews, W.B. Subcortical somatosensory evoked potentials in normal man and in patients with central nervous system lesions. In: J.E. Desmedt (Ed.), Clinical Uses of Cerebral, Brainstem and Spinal Somato-

sensory Evoked Potentials, Progr. clin. Neurophysiol., Vol. 7. Karger, Basel, 1980: 190—204.

Sprague, J.M. and Hong Chien Ha The terminal fields of dorsal root fibers in the lumbosacral spinal cord of the cat, and the dendrite organization of the motor nuclei. Progr. Brain Res., 1964, 11: 120—154.

Sterling, P. and Kuypers, H.G.J.M. Anatomical organization of the brachial spinal cord of the cat. The distribution of dorsal root fibers. Brain Res., 1967, 4: 1—15.

Symon, L., Hargadine, J., Zawirski, M. and Branston, N. Central conduction time as an index of ischemia in subarachnoid haemorrhage. J. neurol. Sci., 1979, 44: 95—103.

Uddenberg, N. Differential localization in dorsal funiculus of fibres originating from different receptors. Exp. Brain Res., 1968, 4: 367—376.

Wall, P.D. Dorsal horn electrophysiology. In: A. Iggo (Ed.), Handbook of Sensory Physiology, Vol. 2. Springer, Berlin, 1973: 253—270.

Wiederholt, W.C. Early components of the somatosensory evoked potential in man, cat and rat. In: J.E. Desmedt (Ed.), Clinical Uses of Cerebral, Brainstem and Spinal Somatosensory Evoked Potentials, Progr. clin. Neurophysiol., Vol. 7. Karger, Basel, 1980: 105—117.

Willis, W.D. and Coggeshall, R.E. Sensory Mechanisms of the Spinal Cord. Wiley, New York, 1978: 485 pp.